JACS
JOURNAL OF THE AMERICAN CHEMICAL SOCIETY
Communication
pubs.acs.org/JACS

Microtesla SABRE Enables 10% Nitrogen-15 Nuclear Spin Polarization

Thomas Theis,*[,†,∥] Milton L. Truong,[‡,∥] Aaron M. Coffey,[‡] Roman V. Shchepin,[‡] Kevin W. Waddell,[‡] Fan Shi,[§] Boyd M. Goodson,[§] Warren S. Warren,[†] and Eduard Y. Chekmenev*[,‡]

[†]Department of Chemistry, Duke University, Durham, North Carolina 27708, United States
[‡]Department of Radiology, Vanderbilt University, Institute of Imaging Science, Nashville, Tennessee 37232, United States
[§]Department of Chemistry and Biochemistry, Southern Illinois University, Carbondale, Illinois 62901, United States

Supporting Information

ABSTRACT: Parahydrogen is demonstrated to efficiently transfer its nuclear spin hyperpolarization to nitrogen-15 in pyridine and nicotinamide (vitamin B_3 amide) by conducting "signal amplification by reversible exchange" (SABRE) at microtesla fields within a magnetic shield. Following transfer of the sample from the magnetic shield chamber to a conventional NMR spectrometer, the ^{15}N NMR signals for these molecules are enhanced by ~30,000- and ~20,000-fold at 9.4 T, corresponding to ~10% and ~7% nuclear spin polarization, respectively. This method, dubbed "SABRE in shield enables alignment transfer to heteronuclei" or "SABRE-SHEATH", promises to be a simple, cost-effective way to hyperpolarize heteronuclei. It may be particularly useful for in vivo applications because of longer hyperpolarization lifetimes, lack of background signal, and facile chemical-shift discrimination of different species.

The traditional limitation of magnetic resonance (MR) is low sensitivity because of low thermal equilibrium polarization (P ~10^{-5}–10^{-6}). This limitation can be overcome by hyperpolarized magnetic resonance (HP-MR), which can boost P by several orders of magnitude. In addition, HP-MR is sensitive to molecular changes (reported by the chemical shift) and is free of ionizing radiation (unlike the established molecular imaging methods PET or SPECT). Thus, HP-MR enables real-time tracking of metabolic pathways and distribution processes.[1−4] Moreover, HP-MR works for drugs and metabolites in their natural form, free of cumbersome radioactive labels that alter biological function. These unique features of HP-MR create new avenues for interrogating disease states, their aggressiveness, degree of progression, and response to treatment.[5−7]

To date, most biomedical HP-MR applications involve dissolution dynamic nuclear polarization (d-DNP).[1−7] However, d-DNP is associated with high costs and lengthy hyperpolarization times: P ~70% polarization in 20 min under optimal conditions.[9] An alternative, cost-effective, and continuous source of hyperpolarization is "Signal Amplification By Reversible Exchange" (SABRE), which uses parahydrogen (*para*-H_2) as the source of spin order.[10] SABRE employs an organometallic catalyst that transiently binds both *para*-H_2 and target molecules, permitting the transfer of spin order from *para*-H_2 to the target by matching the resonance frequency difference between *para*-H_2 and protons on the target to the magnitude of through-bond J-couplings. (Typically, the optimal B_0 is ~5−8 mT).[11] The main limitation of SABRE is the requirement for transient binding on a catalyst which currently restricts the potential classes of molecules amenable to SABRE. Nevertheless, a number of pyridine derivatives (e.g., nicotinamide,[10] pyrazinamide, and isoniazid)[12] and DNA building blocks (e.g., adenine and adenosine)[13] have been successfully hyperpolarized. Another significant limitation of SABRE is that it has been primarily used to hyperpolarize protons, which depolarize quickly (typically in seconds), making metabolic tracking on biologically relevant time scales challenging; direct detection of ^1H signals also competes with background signals from water. Heteronuclear spins like ^{15}N have lower sensitivity but are attractive because they have long polarization lifetimes, which in special cases can exceed 10 min.[14] SABRE-derived proton hyperpolarization has recently been transferred to ^{13}C, but, thus far, the associated efficiency remains low (P ~0.03%)—a significant enhancement, but one that leaves room for improvement.[15] Such recent improvements include "high-field SABRE" (via incoherent polarization transfer), which removes the need for sample transfer from the polarization region to the magnet for detection[16] (relying on incoherent polarization transfer in its first demonstration). This was improved again by enabling coherent transfer of *para*-H_2 polarization to targets at high field using rf irradiation and shown to work for ^1H as well as for ^{15}N.[17−19]

Here we demonstrate direct production of P ~10% on ^{15}N by SABRE, exceeding all previous demonstrations by orders of magnitude. We use a field cycling strategy down to extremely low magnetic fields (~μT) known to transfer *para*-H_2-derived hyperpolarization to heteronuclei in hydrogenative *para*-H_2 induced polarization.[11,15,18,20−31] We call the presented hyperpolarization strategy SABRE in SHield Enables Alignment Transfer to Heteronuclei (SABRE-SHEATH), which we demonstrate using ^{15}N-Py and ^{15}N-nicotinamide, but immediately extends to other ^{15}N enriched heterocyclic compounds. Py,[32,33] nicotinamide,[34] and others[32,35] can be enriched with ^{15}N using simple chemistries that allow either direct heteroatom replacement[32,35] or through ring opening and closure[33] using $^{15}NH_4Cl$[32−35] as a cheap spin label source. As a result, the labor-intensive synthesis of complex ^{15}N-labeled biomolecules can be largely avoided for this class of heterocycles. Correspondingly, our theoretical analysis easily extends to other biologically

Received: November 30, 2014
Published: January 13, 2015

DOI: 10.1021/ja512242d
J. Am. Chem. Soc. 2015, 137, 1404−1407

relevant molecules already shown to be amenable to ^{1}H SABRE hyperpolarization.

The presented experiments shine in their simplicity: *para*-H_2 is bubbled through a methanol-d_4 solution containing activated catalyst ($[IrH_2(^{15}N\text{-}Py)_3(IMes)]^+$) and ^{15}N-Py inside a μ-metal magnetic shield where the hyperpolarization is created; see Figure 1A. Subsequently, the sample is transferred into an NMR

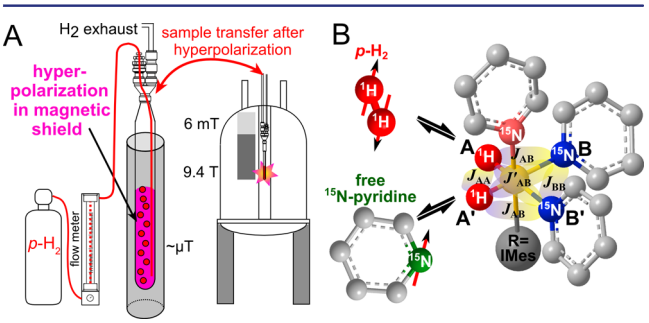

Figure 1. Setup for the SABRE-SHEATH experiment. (A) shows the sample in an NMR tube held inside the μ-metal shield, where *para*-H_2 is bubbled through the solution. After hyperpolarization the sample is transferred into NMR spectrometer for detection. (B) *para*-H_2 and ^{15}N-pyridine (^{15}N-Py) in exchange with $[IrH_2(^{15}N\text{-}Py)_3(IMes)]^+$. On the catalyst *para*-H_2 transfers its hyperpolarization to ^{15}N-Py through the *J*-coupling network. The equatorial ^{15}N-Py (blue) is in fast exchange and responsible for the hyperpolarization of the free ^{15}N-Py (green).

magnet for detection after a 90° pulse. The in-phase nature of the resulting signal is of particular importance for imaging applications, where the associated broader lines would suffer signal cancellations if the signals were antiphase.[37]

The simplest model for SABRE hyperpolarization uses the quantum mechanics of AA′BB′ systems developed in 1957 by Pople et al.[38] Such an AA′BB′ spin system is formed in the catalytic intermediate $[IrH_2(^{15}N\text{-}Py)_3(IMes)]^+$, as illustrated in Figure 1A. The AA′BB′ system consists of the *para*-H_2 protons (AA′) and the ^{15}N-nuclei of the two Py (BB′) in the equatorial plane. The spectral features of importance are the Larmor frequencies ν_A of ^{1}H, ν_B of ^{15}N, and the spin couplings $J_{AA'}$, $J_{BB'}$, $J_{AB} = J_{A'B'}$, and $J_{AB'} = J_{A'B}$. At specific magnetic fields different sets of energy levels of the AA′BB′ system are brought very close to one another (they experience anticrossing),[20,21] thereby permitting efficient polarization transfer from the A-spins to the B-spins.

Building on previous work discussing the importance of low fields for efficient polarization transfer from *para*-H_2 to heteronuclei,[11,15,18,20−28] the Supporting Information (SI) provides a theoretical description of the polarization-transfer process. In the SI it is shown that the hyperpolarization process can be intuitively understood as simple rotations on a Blochsphere. This theoretical analysis shows that generally, $\Delta\nu = \nu_A - \nu_B$ needs to match one of the following *J*-terms:

$$J_{1T} = \pm(J_{AA} - J_{BB})$$
$$J_{2T} = \pm(J_{AA} + J_{BB} - (J_{AB} + J'_{AB})/2) \quad (1)$$

When $\Delta\nu = +J_{1T}$ or J_{2T} hyperpolarization aligned with the weak external magnetic field is created; reversing the direction of the magnetic field matches to the other state and reverses the direction of the induced magnetization. In eq 1 only $\Delta\nu$ depends on the magnetic field, given as

$$\Delta\nu = B_0(\gamma_A(1 - \sigma_A) - \gamma_B(1 - \sigma_B)) \quad (2)$$

where B_0 is the magnetic field in Tesla, γ is the gyromagnetic ratio in MHz/T, and σ is the chemical shielding (in relative units conventionally related to the chemical shift δ (in units of ppm) as $\delta = 10^6 \times (\sigma_{ref} - \sigma_{sample})$, where σ_{ref} and σ_{sample} are the chemical shielding values of the reference sample (i.e., TMS for ^{1}H NMR and liquid $^{15}NH_3$ for ^{15}N) and the sample of interest. Combining eqs 1 and 2 provides the magnetic field for polarization transfer:

$$B_{0\text{-transfer}} = \frac{J_{1T}}{\gamma_A(1 - \sigma_A) - \gamma_B(1 - \sigma_B)} \text{ or } \frac{J_{2T}}{\gamma_A(1 - \sigma_A) - \gamma_B(1 - \sigma_B)} \quad (3)$$

In the original (homonuclear) case for SABRE ($\gamma_A = \gamma_B$), the matching condition is only dependent on the chemical shielding difference $\Delta\sigma = 10^{-6} \times \Delta\delta$) between *para*-$H_2$-derived hydrides, σ_A, and Py protons σ_B. In this case, the optimal B_0 is ~6.6 mT (i.e., $B_{0\text{-transfer}}$ = 9 Hz/0.000032/42.6 MHz/T, assuming $\Delta\delta$ ~32 ppm and J_T ~9 Hz);[11] this magnetic field corresponds to the conditions at which ^{1}H-SABRE is most efficient.[10,37,39,40] For the heteronuclear case—of primary focus here—eq 2 gives a significantly different result: For ^{15}N/^{1}H, an optimal transfer field of $B_{0\text{-transfer}}$ ~0.2−0.4 μT is predicted by eq 3 (assuming $\Delta\gamma$ ~47 MHz/T), depending on the exact value of J_T; note $\Delta\sigma$ is negligible given the large $\Delta\gamma$. However, this condition does not have to be precisely met, as it is limited by the residence times of *para*-H_2 and the substrate molecule (e.g., Py) on the Ir complex, which are typically on the time scale of ~0.1 s.[41] This new target magnetic field is significantly lower than the Earth's magnetic field (~50 μT); thus, ^{15}N-SABRE experiments were conducted in a layer of μ-metal to shield the Earth's magnetic field.

SABRE-SHEATH polarization is demonstrated by placing the NMR tube in a 305 mm-long magnetic shield (Lake Shore Cryotronics, P/N 4065) during ~30 s of bubbling. Note that no attempt was made to tune the small residual field to a precise value. After this ~30 s polarization period, *para*-H_2 delivery is stopped, and the NMR tube is quickly transferred (~4 s) to a 9.4 T NMR spectrometer to detect the SABRE-SHEATH polarization through conventional 1D-NMR. Both ^{15}N and ^{1}H pulse-acquire NMR experiments were conducted (see SI for further experimental details). Figure 2 highlights the main results: At concentrations of 4 mM ^{15}N-Py (and 0.24 mM catalyst), a 30,000-fold polarization enhancement over the thermal level is achieved (Figure 2A). The thermal ^{15}N polarization at 9.4 T and room temperature is ~3.3 × 10^{-6}, thus this enhancement corresponds to a P_{15N} ~10%.

The results obtained with 63 mM ^{15}N-Py (6.3 mM catalyst, Figure 2B) illustrate that with increasing concentrations, the absolute signal can be further increased, but the corresponding enhancement level (and the respective *P*) is diminished to 3000-fold (P ~ 1%). The reduced enhancements observed with increasing concentrations are limited by three factors: (i) the finite amount of dissolved *para*-H_2 limits the available hyperpolarization that can be passed to ^{15}N-Py molecules; (ii) the Ir catalyst and ^{15}N-Py concentrations modulate ^{15}N-Py residence time, which affects the efficiency of SABRE polarization transfer;[40] and (iii) the NHC Ir catalyst is a source of T_1 relaxation.[40] Optimization of these three and other (e.g., temperature and *para*-H_2 pressure) parameters may in principle lead to higher, even on the order of unity, ^{15}N hyperpolarization, which would be particularly important in the context of biomedical translation of this work.

The spectral pattern observed for free ^{15}N-Py molecules in the SABRE-SHEATH experiments (Figures 2A and B) is a clean, emissive in-phase triplet, as expected, because of the dominant

DOI: 10.1021/ja512242d
J. Am. Chem. Soc. 2015, 137, 1404−1407

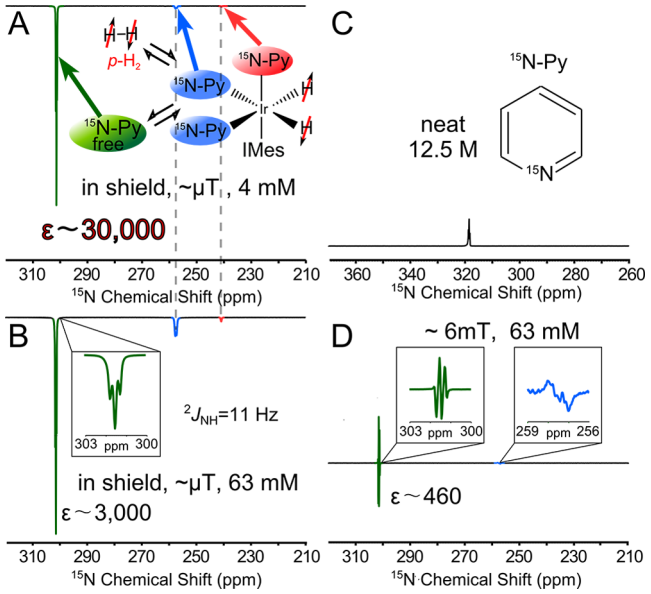

Figure 2. Single-shot ^{15}N NMR SABRE spectra. (A) SABRE-SHEATH experiment with Ir catalyst and ^{15}N-Py concentrations of 0.24 and 4 mM respectively result in 30,000-fold signal enhancement corresponding to P ~10% with ^{15}N T_1 ~ 42 s at 9.4 T. (B) Shows that increase of Ir catalyst and ^{15}N-Py concentrations results in further increased NMR signals, but relative enhancement and P levels decrease. An in-phase triplet split by 11 Hz is observed in both A and B. SABRE-SHEATH experiments (A, B) also reveal both bound ^{15}N-Py ligand site of the activated Ir catalyst. (C) NMR spectrum of neat 12.5 M ^{15}N-Py used for calibration. (D) ^{15}N-SABRE at conditions optimized for ^{1}H hyperpolarization (6 ± 4 mT) results in antiphase triplets and lower enhancements.

two-bond J-coupling between ^{15}N and the *ortho*-Py-protons ($^2J_{NH}$ is ≈11 Hz). In the traditional low-field SABRE experiment (at ~6 mT)[10] optimized for protons, the ^{15}N-triplet is typically characterized not only by lower enhancements but also by purely antiphase signatures, which can make such signals less useful in imaging applications because of partial signal cancellation from spectrally broadened lines.

In the SABRE-SHEATH experiments (Figure 2A,B), not only is the free ^{15}N-Py signal detected, but signals from the ligand-bound species are observed as well. The equatorial ^{15}N-Py molecules in the catalytic intermediate (blue) are those that exchange quickly and produce the observed hyperpolarization of the free ^{15}N-Py (green). The axial ^{15}N-Py (red) is also clearly visible in the SABRE-SHEATH experiments. This axial ^{15}N-Py is no longer detectable in the experiments optimized for ^{1}H SABRE (Figure 2D), where antiphase lines result.[37] The NMR lines of the catalyst-bound species are intrinsically broadened. Thus, the in-phase lines are still easily observable in SABRE-SHEATH experiments (Figure 2A,B), however the experiments conducted at ~6 ± 4 mT (Figure 2D) exhibit antiphase lines with reduced enhancements.

The presented theory predicts the observation of in-phase signals resulting from standard I_z-magnetization in the SABRE-SHEATH experiments. We speculate that the antiphase signals in the 6 ± 4 mT experiments arise because the initial singlet spin-order of *para*-H_2 is transferred not only into I_z-magnetization on protons but also into zero-quantum terms (e.g., $ZQ_x = I_{1x}I_{2x} + I_{1y}I_{2y}$) on pairs of Py-protons, which are finally transferred (by the $^2J_{NH}$-coupling $\propto I_zS_z$) into antiphase terms between protons and ^{15}N (e.g., $I_{1z}I_{2z}S_y$), thereby resulting in antiphase signals. Additional indication for the involvement of antiphase and zero-quantum terms are presented in the the SI.

We also point out that polarization transfer strategies, e.g., ^{1}H → ^{15}N via INEPT, are unlikely to be as effective as the direct ^{15}N-hyperpolarization in the SABRE-SHEATH because, as we demonstrate in the SI, standard proton SABRE is much less effective for ^{15}N-Py than on the natural abundant ^{14}N-Py.

This method can also be applied to other biomolecular contrast agents with ^{15}N spin labels, such as ^{15}N-nicotinamide (vitamin B_3 amide);[12,36] Figure 3A demonstrates an enhancement of ε ~20,000 (%P ~7%) at 48 mM; a significantly higher concentration than that demonstrated for the greatest ^{15}N-Py enhancement and potentially suitable for biomedical applications. Future demonstrations will likely show SABRE-SHEATH to work with heterogeneous catalysts[42] and/or in aqueous media[15,43] bringing this technique closer to its ultimate applications.

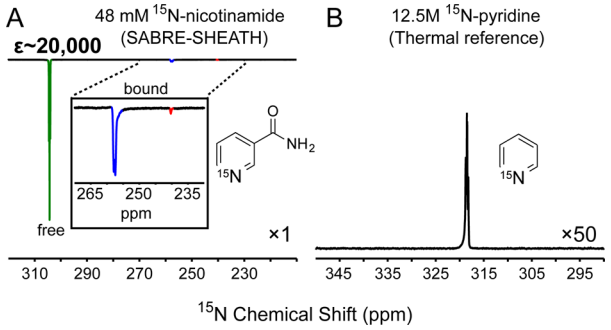

Figure 3. (A) ^{15}N SABRE-SHEATH of a 48 mM sample of ^{15}N-nicotinamide (^{15}N enrichment of ~66%) in methanol-d_4 using 2 mM of activated IMes catalyst. An enhancement ε of ~20,000-fold (corresponding to %P_{15N} ~ 7%) was achieved in comparison to (B) a spectrum of thermally polarized sample of 12.5 M ^{15}N-Py (note the vertical axis is scaled by 50 fold). The spectrum of HP ^{15}N-nicotinamide shows the expected three resonances of free and bound species. See SI for details.

In conclusion, a simple and cost-effective hyperpolarization scheme to produce high P levels on heteronuclei has greater T_1 (P^{15}N ~10%) is developed by conducting SABRE experiments with a ^{15}N-labeled substrate in a magnetic shield. Despite the requirement for isotopic labeling, the heterocyclic compounds currently amenable to SABRE are well suited for inexpensive and straightforward enrichment strategies. The resulting hyperpolarization on heteronuclei, which are likely required for tracing hyperpolarized biomarkers *in vivo*. This technique can easily be extended to other biomolecules bearing ^{15}N in important Py derivatives, but it is to be expected that many other classes of molecules will be enabled given the rapid progress in the field, and SABRE-SHEATH will likely remain an advantageous method to polarize heteronuclei including ^{15}N and ^{13}C. Future applications span from biomolecular imaging, to the study of protein dynamics.

■ ASSOCIATED CONTENT

Supporting Information

Additional experimental details; theoretical analysis of hyperpolarization transfer. This material is available free of charge via the Internet at http://pubs.acs.org.

DOI: 10.1021/ja512242d
J. Am. Chem. Soc. 2015, 137, 1404−1407

AUTHOR INFORMATION

Corresponding Authors

*thomas.theis@duke.edu
*eduard.chekmenev@vanderbilt.edu

Author Contributions

‖These authors contributed equally

Notes

The authors declare no competing financial interest.

ACKNOWLEDGMENTS

F.S and B.M.G. thank K. N. Plunkett (SIUC) and his research group for glovebox access and other resources and for previous assistance with catalyst synthesis. We thank Dr. Panayiotis Nikolaou for help with TOC graphics. This work was supported by NSF under grants CHE-1058727, CHE-1363008, CHE-1416268, NIH 1R21EB018014 and 2R15EB007074, and by the DOD CDMRP breast cancer W81XWH-12-1-0159/BC112431.

REFERENCES

(1) Kurhanewicz, J.; Vigneron, D. B.; Brindle, K.; Chekmenev, E. Y.; Comment, A.; Cunningham, C. H.; Deberardinis, R. J.; Green, G. G.; Leach, M. O.; Rajan, S. S.; Rizi, R. R.; Ross, B. D.; Warren, W. S.; Malloy, C. R. *Neoplasia* **2011**, *13*, 81.

(2) Nelson, S. J.; Kurhanewicz, J.; Vigneron, D. B.; Larson, P. E. Z.; Harzstark, A. L.; Ferrone, M.; van Criekinge, M.; Chang, J. W.; Bok, R.; Park, I.; Reed, G.; Carvajal, L.; Small, E. J.; Munster, P.; Weinberg, V. K.; Ardenkjaer-Larsen, J. H.; Chen, A. P.; Hurd, R. E.; Odegardstuen, L. I.; Robb, F. J.; Tropp, J.; Murray, J. A. *Sci. Transl. Med.* **2013**, *5*, 198ra108.

(3) Brindle, K. M.; Bohndiek, S. E.; Gallagher, F. A.; Kettunen, M. I. *Magn. Reson. Med.* **2011**, *66*, 505.

(4) Merritt, M. E.; Harrison, C.; Sherry, A. D.; Malloy, C. R.; Burgess, S. C. *Proc. Natl. Acad. Sci. U. S. A.* **2011**, *108*, 19084.

(5) Keshari, K. R.; Wilson, D. M.; Sai, V.; Bok, R.; Jen, K.-Y.; Larson, P.; Van Criekinge, M.; Kurhanewicz, J.; Wang, Z. J. *Diabetes* **2014**, DOI: 10.2337/db13.

(6) Day, S. E.; Kettunen, M. I.; Gallagher, F. A.; Hu, D. E.; Lerche, M.; Wolber, J.; Golman, K.; Ardenkjaer-Larsen, J. H.; Brindle, K. M. *Nat. Med.* **2007**, *13*, 1382.

(7) Albers, M. J.; Bok, R.; Chen, A. P.; Cunningham, C. H.; Zierhut, M. L.; Zhang, V. Y.; Kohler, S. J.; Tropp, J.; Hurd, R. E.; Yen, Y.-F.; Nelson, S. J.; Vigneron, D. B.; Kurhanewicz, J. *Cancer Res.* **2008**, *68*, 8607.

(8) Jannin, S.; Bornet, A.; Melzi, R.; Bodenhausen, G. *Chem. Phys. Lett.* **2012**, *549*, 99.

(9) Kumagai, K.; Kawashima, K.; Akakabe, M.; Tsuda, M.; Abe, T.; Tsuda, M. *Tetrahedron* **2013**, *69*, 3896.

(10) Adams, R. W.; Aguilar, J. A.; Atkinson, K. D.; Cowley, M. J.; Elliott, P. I. P.; Duckett, S. B.; Green, G. G. R.; Khazal, I. G.; Lopez-Serrano, J.; Williamson, D. C. *Science* **2009**, *323*, 1708.

(11) Adams, R. W.; Duckett, S. B.; Green, R. A.; Williamson, D. C.; Green, G. G. R. *J. Chem. Phys.* **2009**, *131*, 194505.

(12) Zeng, H.; Xu, J.; Gillen, J.; McMahon, M. T.; Artemov, D.; Tyburn, J.-M.; Lohman, J. A. B.; Mewis, R. E.; Atkinson, K. D.; Green, G. G. R.; Duckett, S. B.; van Zijl, P. C. M. *J. Magn. Reson.* **2013**, *237*, 73.

(13) Hovener, J. B.; Schwaderlapp, N.; Lickert, T.; Duckett, S. B.; Mewis, R. E.; Highton, L. A. R.; Kenny, S. M.; Green, G. G. R.; Leibfritz, D.; Korvink, J. G.; Hennig, J.; von Elverfeldt, D. *Nat. Commun.* **2013**, *4*, 5.

(14) Nonaka, H.; Hata, R.; Doura, T.; Nishihara, T.; Kumagai, K.; Akakabe, M.; Tsuda, M.; Ichikawa, K.; Sando, S. *Nat. Commun.* **2013**, *4*, 2411.

(15) Hövener, J.-B.; Schwaderlapp, N.; Borowiak, R.; Lickert, T.; Duckett, S. B.; Mewis, R. E.; Adams, R. W.; Burns, M. J.; Highton, L. A. R.; Green, G. G. R.; Olaru, A.; Hennig, J.; von Elverfeldt, D. *Anal. Chem.* **2014**, *86*, 1767.

(16) Barskiy, D. A.; Kovtunov, K. V.; Koptyug, I. V.; He, P.; Groome, K. A.; Best, Q. A.; Shi, F.; Goodson, B. M.; Shchepin, R. V.; Coffey, A. M.; Waddell, K. W.; Chekmenev, E. Y. *J. Am. Chem. Soc.* **2014**, *136*, 3322.

(17) Theis, T.; Truong, M.; Coffey, A. M.; Chekmenev, E. Y.; Warren, W. S. *J. Magn. Reson.* **2014**, *248*, 23.

(18) Pravdivtsev, A. N.; Yurkovskaya, A. V.; Vieth, H.-M.; Ivanov, K. L.; Kaptein, R. *ChemPhysChem* **2013**, *14*, 3327.

(19) Pravdivtsev, A. N.; Yurkovskaya, A. V.; Vieth, H.-M.; Ivanov, K. L. *Phys. Chem. Chem. Phys.* **2014**, *16*, 24672.

(20) Buljubasich, L.; Franzoni, M. B.; Spiess, H. W.; Münnemann, K. *J. Magn. Reson.* **2012**, *219*, 33.

(21) Franzoni, M. B.; Buljubasich, L.; Spiess, H. W.; Munnemann, K. *J. Am. Chem. Soc.* **2012**, *134*, 10393.

(22) Colell, J.; Türschmann, P.; Glöggler, S.; Schleker, P.; Theis, T.; Ledbetter, M.; Budker, D.; Pines, A.; Blümich, B.; Appelt, S. *Phys. Rev. Lett.* **2013**, *110*, 137602.

(23) Theis, T.; Feng, Y.; Wu, T.; Warren, W. S. *J. Chem. Phys.* **2014**, *140*, 014201.

(24) Turschmann, P.; Colell, J.; Theis, T.; Blumich, B.; Appelt, S. *Phys. Chem. Chem. Phys.* **2014**, *16*, 15411.

(25) Kiryutin, A. S.; Ivanov, K. L.; Yurkovskaya, A. V.; Kaptein, R.; Vieth, H. M. *Z. Phys. Chem.* **2012**, *226*, 1343.

(26) Theis, T.; Ledbetter, M. P.; Kervern, G.; Blanchard, J. W.; Ganssle, P. J.; Butler, M. C.; Shin, H. D.; Budker, D.; Pines, A. *J. Am. Chem. Soc.* **2012**, *134*, 3987.

(27) Theis, T.; Ganssle, P.; Kervern, G.; Knappe, S.; Kitching, J.; Ledbetter, M. P.; Budker, D.; Pines, A. *Nat. Phys.* **2011**, *7*, 571.

(28) Feng, Y.; Theis, T.; Wu, T.-L.; Claytor, K.; Warren, W. S. *J. Chem. Phys.* **2014**, *141*, 134307.

(29) Reineri, F.; Viale, A.; Giovenzana, G.; Santelia, D.; Dastru, W.; Gobetto, R.; Aime, S. *J. Am. Chem. Soc.* **2008**, *130*, 15047.

(30) Golman, K.; Axelsson, O.; Johannesson, H.; Mansson, S.; Olofsson, C.; Petersson, J. S. *Magn. Reson. Med.* **2001**, *46*, 1.

(31) Bowers, C. R.; Weitekamp, D. P. *Phys. Rev. Lett.* **1986**, *57*, 2645.

(32) Fărcaşiu, D.; Lezcano, M. *J. Labelled Compd. Radiopharm.* **2013**, *56*, 637.

(33) Whaley, T. W.; Ott, D. G. *J. Labelled Compd. Radiopharm.* **1974**, *10*, 283.

(34) Oppenheimer, N. J.; Matsunaga, T. O.; Kam, B. L. *J. Labelled Comp. Radiopharm.* **1978**, *15*, 191.

(35) Schippers, N.; Schwack, W. *J. Labelled Comp. Radiopharm.* **2006**, *49*, 305.

(36) Mewis, R. E.; Atkinson, K. D.; Cowley, M. J.; Duckett, S. B.; Green, G. G. R.; Green, R. A.; Highton, L. A. R.; Kilgour, D.; Lloyd, L. S.; Lohman, J. A. B.; Williamson, D. C. *Magn. Reson. Chem.* **2014**, *52*, 358.

(37) Atkinson, K. D.; Cowley, M. J.; Elliott, P. I. P.; Duckett, S. B.; Green, G. G. R.; Lopez-Serrano, J.; Whitwood, A. C. *J. Am. Chem. Soc.* **2009**, *131*, 13362.

(38) Pople, J. A.; Schneider, W. G.; Bernstein, H. J. *Can. J. Chem.* **1957**, *35*, 1060.

(39) Cowley, M. J.; Adams, R. W.; Atkinson, K. D.; Cockett, M. C. R.; Duckett, S. B.; Green, G. G. R.; Lohman, J. A. B.; Kerssebaum, R.; Kilgour, D.; Mewis, R. E. *J. Am. Chem. Soc.* **2011**, *133*, 6134.

(40) Lloyd, L. S.; Asghar, A.; Burns, M. J.; Charlton, A.; Coombes, S.; Cowley, M. J.; Dear, G. J.; Duckett, S. B.; Genov, G. R.; Green, G. G. R.; Highton, L. A. R.; Hooper, A. J. J.; Khan, M.; Khazal, I. G.; Lewis, R. J.; Mewis, R. E.; Roberts, A. D.; Ruddlesden, A. J. *Catal. Sci. Technol.* **2014**, *4*, 3544.

(41) van Weerdenburg, B. J. A.; Gloggler, S.; Eshuis, N.; Engwerda, A. H. J.; Smits, J. M. M.; de Gelder, R.; Appelt, S.; Wymenga, S. S.; Tessari, M.; Feiters, M. C.; Blumich, B.; Rutjes, F. P. J. T. *Chem. Commun.* **2013**, *49*, 7388.

(42) Shi, F.; Coffey, A. M.; Waddell, K. W.; Chekmenev, E. Y.; Goodson, B. M. *Angew. Chem., Int. Ed.* **2014**, *53*, 7495.

(43) Truong, M. L.; Shi, F.; He, P.; Yuan, B.; Plunkett, K. N.; Coffey, A. M.; Shchepin, R. V.; Barskiy, D. A.; Kovtunov, K. V.; Koptyug, I. V.; Waddell, K. W.; Goodson, B. M.; Chekmenev, E. Y. *J. Phys. Chem. B* **2014**, *18*, 13882.

DOI: 10.1021/ja512242d
J. Am. Chem. Soc. 2015, 137, 1404−1407